PCCP

Hydrogen bonding and the dipole moment of hydrofluorocarbons by density functional theory

Benedito J. Costa Cabral,*[a] Rita C. Guedes,[a] Rahool S. Pai-Panandiker[b] and Carlos A. Nieto de Castro[b]

[a] *Departamento de Química e Bioquímica and Centro de Física da Matéria Condensada, Complexo Interdisciplinar da Universidade de Lisboa, Avenida Prof. Gama Pinto 2, 1649-003 Lisboa, Portugal. E-mail: ben@adonis.cii.fc.ul.pt; rguedes@cii.fc.ul.pt*

[b] *Departamento de Química e Bioquímica and Centro de Ciências Moleculares e Materiais, Faculdade de Ciências da Universidade de Lisboa, Campo Grande, 1749-016 Lisboa, Portugal. E-mail: ccastro@fc.ul.pt; rahool@fc.ul.pt*

Received 29th March 2001, Accepted 26th July 2001
First published as an Advance Article on the web 5th September 2001

Recent measurements of the dielectric permittivity of hydrofluorocarbons in the liquid phase have allowed calculation of the dipole moments in a liquid environment. These values were based on Kirkwood theory, and were significantly greater than the corresponding gas phase dipole moments. In order to understand some features suggesting possible hindered rotation of the molecules in the liquid, density functional and self-consistent-reaction-field calculations for a series of HFC molecules including CHF_2CF_3 (HFC-125), CH_2FCF_3 (HFC-134a), CH_3CF_3 (HFC-143a), CH_2F_2 (HFC-32) and CHF_2CH_3 (HFC-152a) are reported. Particular emphasis has been given to the calculation of dimerisation energies, rotational potentials, polarisabilities and dipole moments. We discuss hydrogen bonding in hydrofluorocarbon dimers and the relationship between the structure and charge distribution of the dimers and the dipole moment in the liquid predicted by relative permittivity measurements. For HFC-32 we have calculated the average dipole moment in small clusters ($n = 2$–10). The structure of the clusters has been determined by density functional theory optimisations ($n = 2$–6) and Monte Carlo simulations ($n = 2$–10). The average dipole moment of the HFC-32 decamer is 2.35 D, which represents a 17% increase relative to the free monomer (2.0 D). We find that the enhancement of the monomer dipole induced by hydrogen bonding in HFC-32 clusters is much less pronounced in comparison with the considerable increase (50%) observed in water clusters.

1. Introduction

The hydrofluorocarbons (HFCs) have become very important in the field of atmospheric chemistry and are technologically very important as replacements for the ozone depleting chlorofluorocarbons (CFCs) and the intermediate hydrochlorofluorocarbons (HCFCs). Study of the electrical properties of these polar fluids, not only gives operational values for the design parameters for the machinery used in air-conditioning and refrigeration, but also provides fascinating insight into their electronic structure. Many experimental studies on these systems have been carried out. Thermodynamic,[1–3] transport properties,[4–7] dielectric measurements[8–12] and spectroscopy[13,14] have all been studied in an attempt to elucidate the liquid state structure of these systems. More recent studies have focussed on dielectric measurements in the liquid state[12,15–18] and the interpretation of neutron scattering spectral data in conjunction with molecular dynamics simulations.[19–21] Several computer simulations based on effective pair-potentials for HFCs have been reported.[22–26]

On the other hand, relatively few quantum mechanical studies on the alternative refrigerants exist in the literature. However, *ab initio* calculations at the Hartree–Fock[27–30] and second-order Møller–Plesset levels,[29,30] have been reported. The more recent studies have focussed on the prediction of vibrational properties,[28,29] polarisabilities and dipole moments.[31] A very recent evaluation of heats of formation of hydrofluorocarbons at the GAUSSIAN-3 (G3) level has been reported.[32]

Recent measurements of the relative permittivity of the haloethane derivatives in the liquid state have allowed calculation of the dipole moments in the liquid. These values were extracted from Kirkwood theory,[33] and are seen to be significantly greater than the dipole moments of the same molecules in the gas phase.[15] This has raised issues regarding the structure, charge distribution of the molecules, and the local order in the liquid state. Moreover, *ab initio* calculations of the average dipole in water clusters[34] and recent first principles simulation of liquid water[35] have indicated that previous effective dipole moments used in classical simulations were possibly underestimated. These theoretical studies have been confirmed by X-ray diffraction measurements with synchrotron radiation which provided an experimental estimation of the dipole moment of liquid water.[36]

In order to improve the analysis and interpretation of the relative permittivity measurements and the prediction of the effective dipole moment in the liquid phase, we report density functional theory (DFT) results for HFC compounds which include CHF_2CF_3 (HFC-125 or **125**), CH_2FCF_3 (HFC-134a or **134a**), CH_3CF_3 (HFC-143a or **143a**), CH_2F_2 (HFC-32 or **32**) and CHF_2CH_3 (HFC-152a or **152a**).

Particular emphasis is placed on the conformational equilibrium related to internal rotation, and on the structure and energetics of HFC dimers. Self-consistent-reaction-field calculations (SCRF) in a dielectric medium representing the liquid

 DOI: 10.1039/b102879k

environment are also reported. In order to analyse polarisation effects related to hydrogen bonding and to estimate the dipole moment of HFC clusters, DFT optimisations and Monte Carlo simulations for small HFC-32 clusters have been carried out. For the most stable clusters, the charge distribution and the average monomer dipole on each cluster have been determined by DFT calculations. We compare our results on HFC clusters with *ab initio* calculations for water clusters[34] which show a significant increase in the average monomer dipole as a function of the cluster size leading to an estimation of the average dipole in the water hexamer (2.7 D)[34] in good agreement with the experimental value for bulk water of 2.9 ± 0.6 D.[36]

2. Experimental evidence

Comprehensive studies of the relative permittivity measurements in the liquid phase and the subsequent treatment of the data to interpret the results have recently been conducted.[12,15–17] The data treatment involves application of the Kirkwood theory[33] for the calculation of the apparent dipole moments μ_K^* in the liquid state, both for pure HFC fluids and for mixtures, and the interpretation of the Kirkwood correlation factor g_K, in the light of possible hindered rotations.[15] Experimental data for the present HFC series are reported in Table 1.

The HFCs exhibit gas phase dipole moments (μ_g) in the order (1): **125** < **32** < **134a** < **152a** < **143a** while the values obtained for the liquid phase, based on the Kirkwood theory (μ_K^*) have a slightly different trend (2): **125** < **143a** < **134a** < **32** < **152a**. As a consequence of these differences, the Kirkwood correlation factor g_K, shows interesting behaviour (3): **143a** < **125** < **152a** < **32** < **134a**.

Since g_K, is indicative of the restriction to rotation imposed by a cage of surrounding molecules on a given molecule,[33] the results may suggest that HFC-143a has the greatest rotational mobility in the liquid state, whereas HFC-134a has the greatest rotational hindrance.

Table 1 also reports data for the effective dipole in the liquid (μ_{KF}^*) predicted by the Kirkwood–Frölich equation[33] where the refractive index (n_∞) has been set to the experimental values in the gas phase.[10,11] Although this is a simplification (frequency dependent data for the permittivity of liquid HFCs are apparently not available), these results for μ_{KF}^* suggest that μ_K^* from the Kirkwood theory may have been overestimated. We note that the relationship between the apparent dipole from relative permittivity measurements and the effective dipole moment in the liquid is not direct and involves statistical-mechanical theories of relative permittivity.[33] In this sense, some of the more recent studies on liquid water[34–36] have contributed to a better definition of the meaning and the value of the dipole moment in the liquid state. Basically, the interactions in the condensed phase modify the local charge distribution on each monomer, leading to an average dipole moment which reflects charge fluctuations and polarisation effects. For water, cooperative effects related to hydrogen bonding induce a significant increase in the dipole moment relative to that of the free monomer.[34] For the present series of HFC we anticipate that this effect will be much less pronounced.

3. Computational details

Our calculations were based on density functional theory. This theory is dependent on the specific representation of the exchange-correlation functional and several possibilities are presently available. To represent exchange we have carried out calculations with Becke's three-parameter hybrid method (B3)[37] and with a more recent functional proposed by Gill (G96).[38] Correlation has been included by using the Perdew and Wang (PW91)[39] and the Lee, Yang and Parr functionals (LYP).[40] Several basis sets have been used, including the Dunning–Huzinaga valence double-zeta (D95V(d,p)),[41] and Dunning's correlation consistent basis sets (cc-pVDZ, aug-cc-pVDZ and aug-cc-pVTZ).[42,43]

The internal rotation in HFCs has been analysed by a relaxed energy scan procedure in which only the parameter related to the internal rotation has been fixed. The rotational potentials have been calculated at the B3LYP/cc-pVDZ level. In the calculation of dimerisation energies, finite basis set effects leading to basis set superposition errors (BSSE) have been estimated by the counterpoise method (CP) of Boys and Bernardi.[44]

Quantum chemical calculations based on simplified representations of the solvent are very useful for elucidation of property changes upon solvation. In order to study the change in electric properties, as studied experimentally, as a function of the change in state, from gas to liquid, this work also reports DFT calculations using the SCRF approach. The present SCRF results are based on the polarised continuum model (PCM)[45] and on the self-consistent isodensity polarised continuum model (SCIPCM).[46] The main difference between the two methods is the definition of the shape of the cavity that contains the "solvated" molecule. In the PCM this is based on a geometrical criterium (overlapping spheres). The SCIPCM is a modification of the IPCM method in which the cavity is defined by using an electronic isodensity surface. In the SCIPCM, this surface is constructed in a self-consistent way. The relative permittivities were those recently reported by Nieto de Castro and co-workers for the liquid state.[12,15–17]

Monte Carlo simulations for HFC-32 clusters have been carried out with an effective pairwise additive potential.[26] This model has been designed to reproduce liquid state properties, including densities and vaporisation enthalpies in good agreement with experiment.[26] We have generated small HFC-32 clusters with $n = 2$–10, where n is the number of molecules. The temperature has been lowered gradually from 200–50 K, and 10^5 moves per molecule have been performed after equilibration at the lower temperature. From the set of generated

Table 1 Experimental dipole moments, polarisabilities and relative permittivities of HFCs. μ_K^* (in D) is the apparent dipole moment in the liquid from Kirkwood theory and g_K is the Kirkwood correlation factor. μ_{KF}^* (in D) is the dipole moment in the liquid from the Kirkwood–Frölich equation and μ_g (in D) is the dipole moment in the gas. ε is the relative permittivity in the liquid and $\varepsilon_\infty \equiv n_\infty^2$, where n_∞ is the experimental refractive index in the gas. α_e (in Å^3) is the average electronic polarisability

	μ_K^{*} [12,15–17]	g_K [12,15–17]	μ_{KF}^*	μ_g [10,11]	ε [12,15–17]	ε_∞ [10,11]	α_e [10,11]
HFC-125	2.48	2.46	1.84	1.56	6.0[a]	1.37	4.36
HFC-134a	3.54; 3.30[18]	3.44	2.67	2.06	18.0[b]	1.45	4.32
HFC-143a	3.34	2.04	2.63	2.34	15.0[c]	1.39	4.04
HFC-32	3.60	3.31	2.61	1.98	23.0[d]	1.39	2.65
HFC-152a	3.69	2.67	2.55	2.26	13.0[e]	1.51	4.24

[a] $d = 1353$ kg m^{-3}; $T = 303$ K. [b] $d = 1474$ kg m^{-3}; $T = 218$ K. [c] $d = 1153$ kg m^{-3}; $T = 233$ K. [d] $d = 1175$ kg m^{-3}; $T = 243.6$ K. [e] $d = 950$ kg m^{-3}; $T = 288.3$ K.

configurations the lower energy structure has been determined and a single-point energy DFT calculation carried out. The total dipoles of the clusters and the monomer dipoles have been calculated from the atomic charge distributions, which have been fitted to the electrostatic potential by using the Merz–Kollman–Singh scheme.[47,48] This scheme gives multipole moments in good agreement with those calculated directly from the wave functions.[49] For some clusters ($n = 3$–6) the structures have been fully optimised by DFT at the B3LYP/D95V(d,p) level and were characterised as local minima, *i.e.*, we have verified that all frequencies are real. SCRF calculations for dimers and clusters were based on the PCM[45] method.

The DFT calculations have been carried out with the GAUSSIAN-98 program.[50]

4. Results and discussion

4.1 Monomers

4.1.1 Structure. Fig. 1 shows the staggered conformers of the four ethane-based compounds. Data for some structural parameters from geometry optimisations at the B3LYP/D95V(d,p) and G96LYP/aug-cc-pVTZ levels are reported in Table 2.

We observe a good agreement between the geometries from the two theoretical levels, indicating that B3LYP/D95V(d,p) optimisations are adequate to predict the geometry of the present compounds. Experimental structures for the present set of molecules are apparently not available. Thus, comparison is made with a single reference molecule. Table 2 reports some experimental data for $C_2H_3F_3$.[51] We observe excellent agreement between experiment and our results, particularly for HFC-125 and HFC-134a. The small reduction in the C–C bondlength for HFC-143a and HFC-152a in comparison with the two other compounds reflects the replacement of fluorine atoms by hydrogen atoms that also induces a small decrease of the A–F–C–F valence angles. SCRF calculations indicate that there is no noticeable change in the condensed phase geometries in comparison with gas phase data.

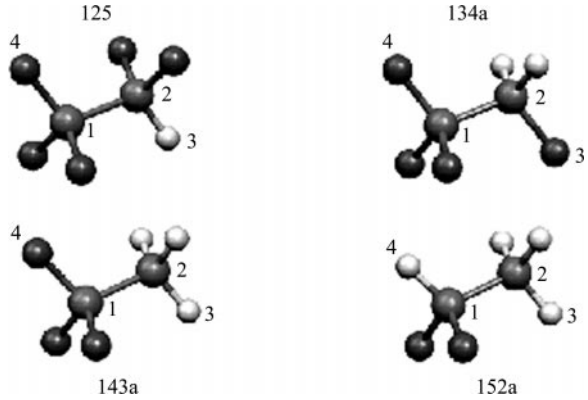

Fig. 1 Staggered conformers of: (a) HFC-125; (b) HFC134a; (c) HFC143a; (d) HFC-152a. The rotation of one group attached to a carbon atom around the vertical plane (4–1–2–3) comprising the C–C bond by an angle ϕ depends on a rotational potential $V(\phi)$. The staggered conformers are the most stable and correspond to $\phi = 180°$.

4.1.2 Dipole and polarisability. Gas phase dipole moments (μ_g) from different theoretical levels are reported in Table 3. In general, excellent agreement between the predictions and the experimental values for the gas phase[10,11] (see Table 1) is observed. Moreover, the experimental order (1) is correctly reproduced by all the theoretical calculations.

Dipole moments in a dielectric medium ($\mu^*(\varepsilon)$) from SCRF calculations are also reported in Table 3. Although SCRF calculations indicate an increase in the dipole moment in the condensed phase, $\mu^*(\varepsilon)$ is significantly lower than μ_K^*. However, a better agreement is observed between SCRF and μ_{KF}^*. Moreover, the order (2) of the dipoles in the liquid, from measurements of the relative permittivity[15] and application of the Kirkwood theory is not reproduced by the SCRF calculations.

Table 2 Structural data of HFCs from density functional geometry optimisations. Bondlengths in Å, valence angles in degrees

	B3LYP/D95V (d,p)	G96LYP/aug-cc-pVTZ	Exp.[a]
125			
C_1–C_2	1.546	1.556	1.45 ± 0.04; 1.53 ± 0.04
C_1–F_4	1.338	1.349	1.330 ± 0.031
C_1–H_3	1.097	1.097	1.093
A–1–2–3	110.4	110.8	
A–2–1–4	111.9	111.9	
A–F–C–F	108.7; 108.4	108.7; 108.2	108.5; 107 ± 3
134a			
C_1–C_2	1.526	1.531	
C_1–F_4	1.354	1.367	
C_2–F_3	1.380	1.393	
A–1–2–3	109.8	110.1	
A–2–1–4	108.7	108.7	
A–F–C–F	107.9; 107.8	107.9; 107.7	
143a			
C_1–C_2	1.509	1.511	
C_1–F_4	1.355	1.368	
C_2–H_3	1.092	1.093	
A–1–2–3	109.4	109.4	
A–2–1–4	111.9	111.9	
A–F–C–F	106.9	106.8	
152a			
C_1–C_2	1.511	1.511	
C_1–H_4	1.097	1.097	
C_2–H_3	1.094	1.094	
A–1–2–3	109.6	109.7	
A–2–1–4	113.9	114.8	
A–F–C–F	107.0	106.7	

[a] Experimental values are for $C_2H_3F_3$ (1,1,1-trifluorethane).[51]

Table 3 Gas phase dipole moments (μ_g in D), effective dipole moment in a dielectric ($\mu^*(\varepsilon)$ in D), effective dipole moment in liquid simulations (μ^*_{eff} in D) and average electronic polarisabilities (α_e in Å^3)

	125	134a	143a	32	152a
μ_g					
B3LYP/D95V(d,p)	1.59	2.11	2.42	2.02	2.34
G96LYP/cc-pVDZ	1.33	1.8	2.12	1.70	1.99
G96LYP/aug-cc-pVDZ	1.52	2.05	2.43	1.96	2.36
G96LYP/aug-cc-pVTZ	1.49	2.01	2.38	1.92	2.32
$\mu^*(\varepsilon)$					
B3LYP/D95V(d,p)[a]	2.1	2.63	2.93	2.36	2.87
B3PW91/D95V(d,p)[b]	1.94	2.61	2.75	2.35	2.77
μ^*_{eff}	1.9[c]	2.24[c]	2.6[d]	2.15[e]; 2.12[f]	2.5[d]
α_e					
G96LYP/aug-cc-pVDZ	5.01	4.85	4.72	2.78	4.66
G96LYP/aug-cc-pVTZ	5.04	4.86	4.72	2.81	4.65

[a] PCM. [b] SCIPCM. [c] Ref. 22. [d] Ref. 23. [e] Ref. 26. [f] Ref. 25.

Effective dipole moments μ^*_{eff} used in the liquid state computer simulations of HFC's[22,26] are also reported in Table 3. They are, in general, even lower than those predicted by SCRF calculations. This feature indicates that the importance of dipolar interactions in the liquid phase has possibly been underestimated by previous intermolecular potential parametrisations.[25,26]

The average dipolar polarisability is $\alpha_e = (\alpha_{xx} + \alpha_{yy} + \alpha_{zz})/3$ and our results for α_e are reported in Table 3. Polarisabilities are very dependent on the basis set. However, we can observe that our results based on aug-cc-pVDZ and aug-cc-pVTZ basis sets are very similar, suggesting that these basis sets are adequate to predict polarisabilities for the present systems. Comparison with experimental results[10,11] (see Table 1) shows a reasonable agreement.

4.1.3 Internal rotation. We are reporting data for the intramolecular potentials related to the rotation around the C–C bond. The most stable conformers correspond to a staggered structure (see Fig. 1). Taking these conformers as reference ones, we call ϕ the angle between the planes defined by the atoms 1–2–3 and 2–1–4 (see Fig. 1). The staggered conformer corresponds to $\phi = 180.0$. Rotation of one group of atoms linked to the same carbon, around the C–C bond involves the rotational barriers represented in Fig. 2. Our results show that the energy barriers are very similar for the different HFC compounds. The intramolecular potentials, calculated at the B3PW91/cc-pVDZ level were fitted to the following expression:

$$V(\phi) = V_o + \sum_{i=1}^{3} V_i[1 - \cos(2i + 1)\phi]$$

The complete set of parameters for the rotational potentials is reported in the caption of Fig. 2, where some literature values[22,23] for the energy barrier V_o between staggered ($\phi = 180.0$) and eclipsed ($\phi = 0.0$) conformers are also indicated. We find good agreement between our predictions and the data for HFC-143a and HFC-152a. However, we observe some significant differences between our barriers and those reported by Lísal and Vacek,[21,22] especially in the case of HFC-134a.

Dipole moments as a function of the angle ϕ are represented in Fig. 3. HFC-125 shows some dependence of the dipole moment on the specific conformation, behaviour also observed in HFC-134a. However, for HFC-143a and HFC-152a the dipole moments are almost independent of ϕ. In all cases, the larger dipole moment corresponds to the most energetically stable staggered conformation. However, in general, the dependence of the dipoles on the conformation is small. This feature is in contrast with experimental studies for other systems, for example, 1,1-dimethoxypropan-2-one,[52] for which

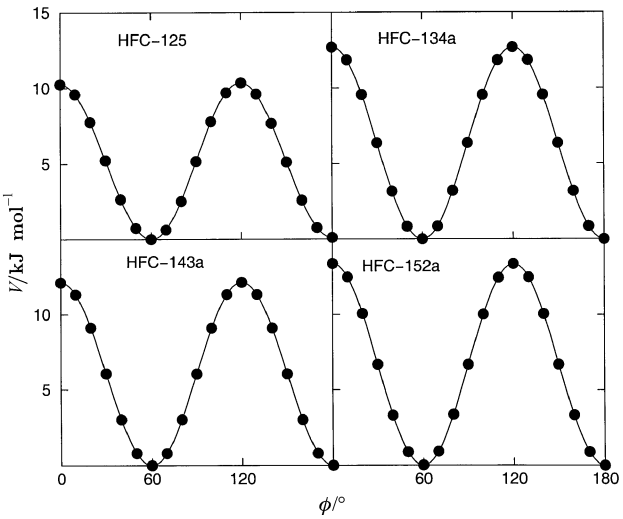

Fig. 2 Rotational potentials for HFCs. Black circles are B3LYP/cc-pVDZ results. Full lines are the fitted potentials represented by: $V(\phi) = V_o + \sum_{i=1}^{3} V_i[1 - \cos(2i + 1)\phi]$. The set of fitted parameters (in kJ mol^{-1}) and literature data[22,23] (in parentheses) for the energy barriers (V_o) are: HFC-125: $V_o = 10.23$ (14.69); $V_1 = -5.1332$; $V_2 = 0.0707$; $V_3 = -0.0002$. HFC-134a: $V_o = 12.71$ (19.16); $V_1 = -6.3511$; $V_2 = -0.0066$; $V_3 = 0.0079$. HFC-143a: $V_o = 12.14$ (13.81); $V_1 = -6.0700$; $V_2 = 0.0011$; $V_3 = -0.0009$. HFC-152a: $V_o = 13.38$ (13.43); $V_1 = -6.6760$; $V_2 = -0.0179$; $V_3 = 0.0085$.

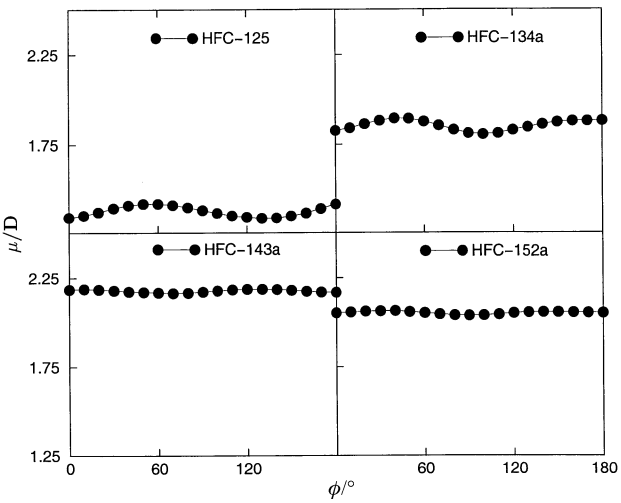

Fig. 3 Dipole moment as a function of the internal rotation around the C–C bond, defined by the angle ϕ. Black circles are results from B3LYP/cc-pVDZ calculations. For HFC-125 and HFC-134a a small dependence of the dipole moment on the angle ϕ is observed.

the overcoming of the potential barrier to free rotation by thermalisation and the corresponding variation of the dipole is invoked to explain the dipole dependence on the temperature.[52] The dipole dependence on the conformation is also important to explain the separation of the isomers HFC-134a and HFC-134 (CF_2HCF_2H) over zeolites.[53]

4.2 Dimers

The accurate determination of the dimer structures is fundamental for a correct parametrisation of intermolecular potential models and although several computer simulations have been reported,[22–26] characterisation of the dimer structures for the present HFC series by *ab initio* or DFT methods appears to be still missing. Moreover, it is reasonable to assume that the orientational order in a liquid is strongly dependent on the structure of the dimers, or small molecular clusters. For the present systems we suggest that some influence of hydrogen bonding on the orientational order and dielectric properties in the liquid phase should be expected.

Fig. 4 shows B3LYP/D95V(d,p) dimer optimised structures. The initial guess for the dimer structures assumed that the dimers are stabilised by hydrogen bond and dipolar interactions. Although no extensive energy surface search has been carried out and other conformations should be expected, the present structures are well characterised minima for which all frequencies are real. In general, the HFC dimers correspond to perpendicular and anti-parallel relative orientation between the two molecules. The perpendicular orientation indicates that dipolar interactions play a secondary role and that the dimer is stabilised by quadrupolar or hydrogen bond interactions. The anti-parallel structure is the second most energetically stable dipolar configuration (the first involves head-to-tail aligned dipoles) and indicates that some features related to the shape or specific directional interactions are also relevant.

The HFC-125 dimer involves two F···H hydrogen bonds of 2.47 and 2.6 Å respectively, and the sum of the van der Waals radii for F···H is 2.55 Å. Our results indicate that the two nearest fluorine atoms, which are those involved in the F···H bonds, are at a distance (F–F) of 3.1 Å. These results are in very good agreement with experimental data for parent systems.[20] For example, from a combined neutron diffraction and molecular dynamics simulation study of trifluoromethane (CHF_3),[20] the peaks of the F–H and F–F radial distribution functions (RDFs) are at 2.6 and 3.1 Å, respectively. We find some differences between our DFT results and molecular dynamics (MD) simulations of liquid HFC-125.[22] From the RDFs, the average F–H and F–F distances are 2.8 and 3.5 Å, respectively. In addition, our H–H distance is 3.7 Å, which is shorter than the average H–H distance from the RDF (4.5 Å). The HFC-125 dimer dipole moment is 0.84 D, indicating a significant reduction relative to the monomer dipole (1.59 D). The two dipole moments on each monomer are 1.66 and 1.64 D respectively, and the angle between the two dipoles is 150°. SCRF single-point energy calculations for the dimer in a dielectric of $\varepsilon = 6.0$ leads to an average dipole of 1.9 D, close to the monomer dipole in the dielectric (2.1 D).

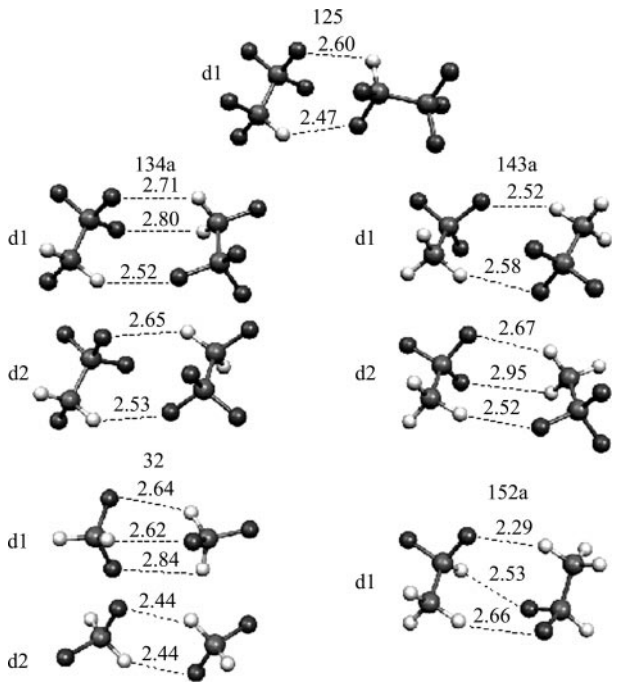

Fig. 4 Dimer structures from B3LYP/D95V(d,p) optimisations for **125** (d1); **134a** (d1 and d2); **143a** (d1 and d2); **32** (d1 and d2); **152a** (d1). F···H distances are in Å.

HFC-134a dimers are characterized by an arrangement with almost anti-parallel orientation between the two molecules. The most stable dimer (d1) involves the formation of three H···F bonds that are in the 2.52–2.80 Å range. These values are in keeping with MD simulations that predict a peak for the F–H RDF at ~2.8 Å.[22] Our F–F distance (3.2 Å) is also in good agreement with the first shell peak of the F–F RDF (~3.5 Å) predicted by MD simulations.[22] The dipole moment of dimer (d1) is 1.78 D, close to the monomer dipole (2.1 D). The monomer dipoles in the dimer are 2.27 D and the angle between them is 131°. The average dipole in the solvated dimer is 2.6 D very similar to the value for the solvated monomer.

The most stable HFC-143a dimer (d1) involves the formation of a double F···H bond of ~2.5 Å. The presence of anti-parallel dimers for this compound is in agreement with results from MD simulations.[23] The dimer dipoles are 0.77 D (d1) and 0.90 D (d2) much lower than that the monomer (2.43 D). The monomer dipoles in d1 are 2.53 and 2.50 D respectively, and the angle between them is 163°. The average monomer dipole in the solvated dimer is 2.89 D, very similar to the value for the solvated monomer (2.93 D).

The HFC-32 dimers correspond to almost perpendicular (d1) and anti-parallel (d2) configurations. In the first structure (d1), the dimer has two F···H pairs separated by 2.6 Å and a third F···H bond of 2.8 Å. This structure corresponds to the most stable dimer reported by Jedlovski and Mezei.[26] The first dimer (d1) has a dipole moment of 2.38 D, higher than the monomer dipole (2.02 D), and the second dimer (d2)) has a dipole moment close to zero. The monomer dipoles in d1 are 2.19 and 2.21 D respectively. The angle between them is 104.7°, in good agreement with the prediction by Jedlovski and Mezei (106°).[26]

The HFC-152a dimer shows two monomers in an almost perpendicular relative orientation. This structure is stabilised by two F···H hydrogen bonds of 2.29 and 2.53 Å respectively, and by a third F···H bond of 2.66 Å. These distances are not in good agreement with the F–H RDF peak position (3.4 Å) predicted by MD simulations.[23] However, we find that the present results are consistent with experimental data[20] and other intermolecular models for HFCs.[20,26] For example, the F–H RDF peak positions in liquid CHF_3 [20] and CH_2F_2 [26] are 2.55 Å, in excellent agreement with our DFT results for the dimer. The dimer dipole is 2.77 D and the monomer dipole is 2.34 D. The average monomer dipole in the dimer is 2.46 D. The angle between the two dipoles is 107.8°. From single-point energy SCRF calculations the average monomer dipole in the solvated dimer is 2.76 D, very similar to the dipole of the solvated monomer (2.87 D).

We find that the total dipoles of the dimers are in the order (4): **125** < **143a** < **134a** < **32** < **152a**. This is the same as sequence (2) that describes the order of the dipoles in the liquid phase and suggests that the formation of hydrogen

bonds between the dimers is relevant in understanding the enhancement of the dipole moment in the liquid phase. We note that the polarisabilities of the dimers are significantly higher than the monomer polarisabilities. For example, at the B3LYP/D95V(d,p) level, the average polarisability of the HFC-152a monomer is 3.6 Å^3 and the dimer polarisability is 7.1 Å^3.

Our F–F distances in HFC dimers are in the 3.4–3.65 Å range. These distances are larger than the experimental value (2.72 Å) in the $(HF)_2$ dimer,[54] reflecting the weaker nature of the hydrogen bond in the HFC compounds. For comparison, we have verified that the $(HF)_2$ dimerisation energy is 17.2 kJ mol^{-1} at the B3LYP/D95V(d,p) level, in good agreement with other theoretical calculations[55,56] (17.6 kJ mol^{-1} at B3LYP/aug-cc-pVTZ)[55] and with the experimental value (~20 kJ mol^{-1}).[57]

Table 4 shows total energies for the HFC monomers (m) and dimers (d). Dimerisation energies (ΔEs) are corrected for zero point vibrational energies and also for BSSE. The CP corrections to BSSE are similar to those found in the studies of hydrogen bonded complexes by DFT.[58] By using the aug-cc-pVTZ basis set, BSSEs are ~1 kJ mol^{-1} for the present HFC series.

The results for the dimerisation energies indicate that the present compounds show relatively weaker hydrogen bonds and very low energy barriers between HFC conformers (~0.5 kJ mol^{-1}), showing that they coexist. Our HFC-32 dimerisation energy is 2.7 kJ mol^{-1} at B3LYP/aug-cc-pVTZ level with BSSE correction. HFC-152a has a dimerisation energy of 3.4 kJ mol^{-1} (B3LYP/aug-cc-pVTZ), which is comparable to the binding energy of $(HCl)_2$ (~5.8–8 kJ mol^{-1}). Thus, our results also suggest that although we can expect the presence of dimers in the liquid state, they may be frequently broken, especially at higher temperatures.

4.3 HFC-32 clusters

HFC-32 clusters (n = 2–10), have been generated by Monte Carlo (MC) simulations at 50 K. For some clusters (n = 2–6) full geometry optimisations at the B3LYP/D95V(d,p) level have been carried out. The initial guess for the optimised structures has been a low energy configuration generated by the MC simulations. Other stable structures corresponding to energy minima should be expected.

Fig. 5 shows the DFT optimised structures for n = 3–6. These calculations indicate a small reduction of some F···H distances from the trimer (2.43 Å) to the hexamer (2.39 Å). This feature indicates some cooperative polarisation effects typical of hydrogen bonding systems.[56] In Fig. 6 (top) we show the average monomer dipole $\langle\mu_i\rangle_n$ as a function of n. We can observe a 10% increase in the dipole from the monomer (2.0 D) to the dimer (2.19 D). For n = 10, $\langle\mu_i\rangle$ = 2.35 D, which is an enhancement of 17% relative to the free monomer (2.0 D) but is substantially lower than the apparent dipole moment μ_K^* from relative permittivity measurements

Table 4 Total energies (in E_h) for the HFC monomers (m) and dimers (d), and dimerisation energies ΔEs (in kJ mol^{-1}). ΔEs include ZPVE corrections at the optimisation level (B3LYP/D95V(d,p)). Values in brackets include counterpoise corrections to BSSE

	B3LYP/aug-cc-pVDZ[a]	B3LYP/aug-cc-pVTZ[a]
125		
m	−576.101 74	−576.262 35
d1	−1152.205 44	−1152.525 98
ΔE	3.94[1.57]	2.15[1.67]
134a		
m	−476.849 87	−476.983 98
d1	−953.702 33	−953.969 18
d2	−953.702 31	−953.969 19
ΔE d1; d2	5.48[3.32]; 5.70[3.5]	2.15[0.89]; 2.20[0.95]
143a		
m	−377.613 83	−377.721 89
d1	−755.229 92	−755.445 44
d2	−755.229 90	−755.445 42
ΔE d1; d2	4.36[2.36]; 4.30[2.09]	2.84[2.18]; 2.83[1.94]
32		
m	−239.018 85	−239.088 29
d1	−478.040 81	−478.178 84
d2	−478.040 49	−478.178 87
ΔE d1; d2	5.54[3.07]; 4.70[3.28]	3.31[2.31]; 3.38[2.67]
152a		
m	−278.347 91	−278.428 38
d1	−556.699 00	−556.859 12
ΔE	6.25[3.83]	4.02[3.23]

[a] Single-point energy calculation. Geometry optimised at B3LYP/D95V(d,p).

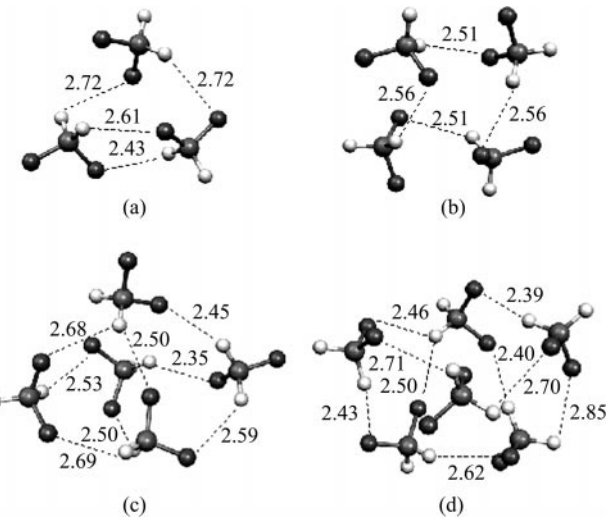

Fig. 5 HFC-32 clusters optimised structures from B3LYP/D95V(d,p) calculations: (a) n = 3; (b) n = 4; (c) n = 5; (d) n = 6. F···H distances in Å.

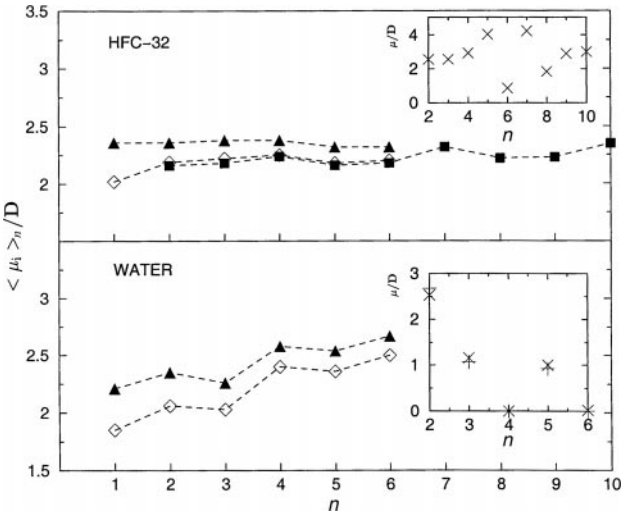

Fig. 6 Average monomer dipole $\langle\mu_i\rangle_n$ and total dipole μ in a cluster as a function of the number of molecules n. Top: HFC-32. B3LYP/D95V(d,p) optimizations (diamonds); B3LYP/D95V(d,p) single-point calculations using Monte Carlo structures (squares); SCRF for the clusters in a dielectric of ε = 23 (triangles). The inset shows the total dipole μ for each cluster in the gas. Bottom: water. B3PW91/aug-cc-pVTZ single-point energy calculations using B3PW91/D95V(d,p) optimised cyclic structures[59] (diamonds); SCRF for the clusters in a dielectric of ε = 78 (triangles). The inset shows the total dipole μ for each cluster in the gas. Plus symbols are *ab initio* results from Gregory *et al.*[34]

(3.6 D).[15] We can also observe excellent agreement between MC and optimised DFT results for $n = 2$–6, which supports the use of the MC procedure for the larger clusters.

The SCRF approach has well known limitations. The more serious concern systems where specific interactions (*e.g.* hydrogen bonds) induce local and significant changes in the electronic density. However, by adding a dielectric medium to a few interacting molecules, it is possible to assess how the presence of this medium affects some molecular properties, for example, the charge distribution. In this way, the more important interactions are explicitly included. In addition, by analysing how the results depend on the number of "solvated" molecules, the limitations of the SCRF approach can be evaluated. Fig. 6 shows SCRF calculations for the HFC-32 clusters. From these calculations, the average monomer dipole in the solvated hexamer is 2.3 D, which is very close to the average monomer dipole in the free decamer (2.35 D), suggesting that SCRF calculations for small clusters provide a realistic description of the charge polarisation for this system. Total dipoles μ for the different clusters (see inset figure) indicate a strong dependence on the cluster size and μ may be very large (*e.g.*, $\mu = 4.2$ D for $n = 7$).

Fig. 6 (bottom) reports data for the average monomer dipole in water clusters. The structures of these clusters have been determined by DFT calculations.[59] The charge distributions are based on single-point energy B3LYP/aug-cc-pVTZ calculations with the geometries optimised at the B3LYP/D95V(d,p) level.[59] The present results are in very good agreement with *ab initio* calculations.[34] We predict that the monomer dipole in small water clusters increases from 1.85 D ($n = 1$) to an average value of 2.5 D ($n = 6$), which is close to the *ab initio* value of 2.7 D.[34] SCRF calculations for the water clusters solvated in a dielectric of $\varepsilon = 78$ show that $\langle\mu_i\rangle_n$ is very dependent on the cluster size. Based on this approach the average monomer dipole (up to the hexamer level) is 2.7 D, in good agreement with recent experimental predictions for bulk water (2.9 ± 0.6 D).[36] Total dipole moments for the different clusters are in excellent agreement with *ab initio* results.[34]

Comparison between the results for the HFC-32 and water clusters shows a much stronger polarisation effect in water. Moreover, the present procedure provides a reliable estimation of the average dipole moment in water clusters, which is similar, in the case of the water hexamer, to the measured dipole moment of bulk water. Thus, our DFT results show that the large dipole moments of HFCs based on relative permittivity measurements and Kirkwood theory cannot be fully explained by polarisation effects induced by hydrogen bonding. Reasons for this discrepancy are possibly related to limitations of the Kirkwood theory and to the eventual formation in the liquid phase, of dimers and small clusters[24] carrying large dipoles (see Fig. 6).

5. Conclusions

Density functional theory results for halogenated hydrocarbons of the ethane series are reported. The compounds studied include HFC-125, HFC-134a, HFC-143a, HFC-32, and HFC-152a.

Gas phase properties are in good agreement with experimental results with respect to the structure and dipole moments. SCRF calculations indicate a significant increase in the dipole moment of HFCs in a continuum medium of relative permittivity corresponding to the liquid state. The effective dipoles from SCRF calculations are much lower than experimental values derived from Kirkwood theory, are in better agreement with predictions based on the Kirkwood–Frölich equation, but are higher than effective dipoles used in computer simulations of HFCs in the liquid phase.[22–26] For HFC-32, our results indicate that the intermolecular potential models used in these simulations[25,26] have possibly underestimated the role played by dipolar interactions and that a polarisable model would certainly be more appropriate to describe local charge fluctuations suggested by DFT calculations for small clusters.

Energy barriers related to internal rotation around the C–C bond for the HFC series in the gas phase are very similar. We found good agreement between our calculations and literature data for the energy barriers related to internal rotations around the C–C bond of HFC-143a and HFC-152a and we have shown that the dipole moments for the present systems are not very dependent on the specific molecular conformation.

We have determined the dimer structures and dimerisation energies for the present series of compounds. The dimer structures are stabilised by double and triple F···H hydrogen bonds, suggesting that these interactions can play a significant role in the liquid state. In addition, our results indicate that the orientational order in the liquid phase may involve not only correlations between the dipoles of monomeric units but also interactions between dimers stabilised by hydrogen bonds. This conclusion is supported by experimental predictions of the apparent dipole moment in the liquid phase based on the Kirkwood theory[15] and by computer simulations of HFC-32[24] indicating the presence of hydrogen bonded stabilised dimers in the liquid phase.

DFT calculations for HFC-32 clusters indicate that the dipole moment of the HFC-32 decamer increases by 17% relative to the free monomer. We find that this effect is significantly smaller than the ~50% increase of the water dipole moment relative to the free monomer predicted by experimental[36] and theoretical studies.[34,35]

Acknowledgements

The authors thank Professor Umesh Mardolcar of Instituto Superior Técnico for sharing unpublished experimental data required in the condensed phase calculations. B.J.C.C., gratefully acknowledges the support of Prof. António Fonseca through the attribution of special computational facilities to R. S. Pai-Panandiker. R. C. Guedes gratefully acknowledges the support of the Fundção para a Ciência e a Tecnologia (FCT) through a PhD grant (PRAXIS XXI/BD/15920/98). This work was partially supported by the SAPIENS Program (Grant No. QUI/35406/99-00), Portugal.

References

1 W. L. Blindenbach, I. G. Economou, P. J. Smits, C. J. Peters and J. D. Arons, *Fluid Phase Equilib.*, 1994, **97**, 13.
2 A. T. Sousa, P. S. Fialho and C. A. Nieto de Castro, *Int. J. Thermophys.*, 1994, **15**, 375.
3 A. T. Sousa, P. S. Fialho, C. A. Nieto de Castro, R. Tufeu and B. Le Neindre, *Int. J. Thermophys.*, 1996, **17**, 551.
4 A. N. Gurova, C. A. Nieto de Castro and U. V. Mardolcar, *Int. J. Thermophys.*, 1997, **18**, 1077.
5 A. N. Gurova, U. V. Mardolcar and C. A. Nieto de Castro, *Int. J. Thermophys.*, 1999, **20**, 63.
6 M. J. Assael, Y. Nagasaka, C. A. Nieto de Castro, R. A. Perkins, K. Ström, E. Vogel and W. A. Wakeham, *Int. J. Thermophys.*, 1995, **16**, 63.
7 M. J. Assael, A. Leipertz, E. MacPherson, Y. Nagasaka, C. A. Nieto de Castro, R. A. Perkins, K. Ström, E. Vogel and W. A. Wakeham, *Int. J. Thermophys.*, 2000, **21**, 1.
8 Y. Tanaka, Y. F. Xiao, S. Matsuo and T. Makita, *Fluid Phase Equilib.*, 1994, **97**, 155.
9 Y. Tanaka and T. Sotani, *Int. J. Thermophys.*, 1996, **17**, 293.
10 C. W. Meyer and G. Morrison, *J. Phys. Chem.*, 1991, **95**, 3860.
11 C. W. Meyer and G. Morrison, *J. Chem. Eng. Data*, 1991, **36**, 409.
12 T. Barão, C. A. Nieto de Castro, U. V. Mardolcar, R. Okambawa and J. M. St-Arnaud, *J. Chem. Eng. Data*, 1995, **40**, 1242.
13 T. E. Mogelberg, O. J. Nielsen, J. Sehested and T. J. Wallington, *J. Phys. Chem.*, 1995, **99**, 13437.
14 I. Merke, J.-U. Grabow, N. Heiniking and W. Stahl, *Z. Naturforsch. A*, 1991, **46**, 799.

15 M. T. Barão, U. V. Mardolcar and C. A. Nieto de Castro, *Int. J. Thermophys.*, 1997, **18**, 419.
16 M. T. Barão, U. V. Mardolcar and C. A. Nieto de Castro, *Fluid Phase Equilib.*, 1998, **150–151**, 753.
17 L. F. Pereira, F. E. Brito, A. N. Gurova, M. T. Barão, U. V. Mardolcar and C. A. Nieto de Castro, *Int. J. Thermophys.*, 2001, in press.
18 A. P. Abbot, C. A. Eardley and R. Tooth, *J. Chem. Eng. Data*, 1999, **44**, 112.
19 K. A. Johnson and W. S. Howells, *J. Phys.: Condens. Matter*, 1999, **11**, 9239.
20 K. A. Mort, K. A. Johnson, D. L. Cooper, A. N. Burgess and W. S. Howells, *Mol. Phys.*, 1997, **90**, 415.
21 K. A. Mort, K. A. Johnson, D. L. Cooper, A. N. Burgess and W. S. Howells, *J. Chem. Soc., Faraday Trans.*, 1998, **94**, 765.
22 M. Lísal and V. Vacek, *Fluid Phase Equilib.*, 1996, **118**, 61.
23 M. Lísal and V. Vacek, *Mol. Phys.*, 1996, **87**, 167.
24 S. Higashi and A. Takada, *Mol. Phys.*, 1997, **92**, 641.
25 S. C. Potter, D. J. Tildesley, A. N. Burgess and S. C. Rogers, *Mol. Phys.*, 1997, **92**, 825.
26 P. Jedlovski and M. Mezei, *J. Chem. Phys.*, 1999, **110**, 2991.
27 T. Sakka, Y. Ogata and M. Iwasaki, *J. Phys. Chem.*, 1992, **96**, 10697.
28 S. J. Paddison, Y. Chen and E. Tschuikow-Roux, *Can. J. Chem.*, 1994, **72**, 561.
29 J. A. Brunelle, L. J. Letendre, E. Weltin, J. H. Brown and C. H. Bushweller, *J. Phys. Chem.*, 1992, **96**, 9225; J. M. Martell and R. S. Boyd, *J. Phys. Chem.*, 1992, **96**, 6287.
30 S. Papasavva, K. H. Illinger and J. E. Kenny, *J. Mol. Struct. (Theochem)*, 1997, **393**, 73; J. M. Martell, R. J. Boyd and Z. Shi, *J. Phys. Chem.*, 1993, **97**, 7208.
31 B. J. Costa Cabral, *J. Mol. Struct. (Theochem)*, 1998, **452**, 117.
32 N. L. Haworth, M. H. Smith, G. B. Bacskay and J. C. Mackie, *J. Phys. Chem.*, 2000, **104**, 7600.
33 C. J. F. Bøttcher, *Theory of Electric Polarization*, Elsevier, Amsterdam, 1973; H. Frölich, *Theory of Dielectrics: Dielectric Constant and Dielectric Loss*, Oxford University Press, London, 1958.
34 J. K. Gregory, D. C. Clary, K. Liu, M. G. Brown and R. J. Saykally, *Science*, 1997, **275**, 814.
35 P. L. Silvestrelli and M. Parrinello, *J. Chem. Phys.*, 1999, **111**, 3572.
36 Y. S. Badyal, M.-L. Saboungi, D. L. Price, S. D. Shastri and D. R. Haeffner, *J. Chem. Phys.*, 2000, **112**, 9206.
37 A. D. Becke, *J. Chem. Phys.*, 1993, **98**, 5648.
38 P. M. W. Gill, *Mol. Phys.*, 1996, **89**, 433.
39 J. P. Perdew and Y. Yang, *Phys. Rev. B*, 1992, **45**, 13244.
40 C. Lee, W. Yang and R. G. Parr, *Phys. Rev. B*, 1988, **37**, 785.
41 T. H. Dunning, Jr.. and P. J. Hay, in *Modern Theoretical Chemistry*, ed. H. F. Schaefer III, Plenum, New York, 1976, vol. 3, p. 1.
42 A. Wilson, T. van Mourik and T. H. Dunning, Jr., *J. Mol. Struct. (Theochem)*, 1997, **388**, 339.
43 D. E. Woon and T. H. Dunning Jr., *J. Chem. Phys.*, 1993, **98**, 1358.
44 S. F. Boys and F. Bernardi, *Mol. Phys.*, 1970, **19**, 553.
45 S. Miertus and J. Tomasi, *Chem. Phys.*, 1982, **65**, 239; V. Barone, M. Cossi and J. Tomasi, *J. Comput. Chem.*, 1998, **19**, 404; V. Barone and M. Cossi, *J. Phys. Chem. A*, 1998, **102**, 1995.
46 J. B. Foresman, T. A. Keith, K. B. Wiberg, J. Snoonian and M. J. Frisch, *J. Phys. Chem.*, 1996, **100**, 16098.
47 U. C. Singh and P. A. Kollman, *J. Comput. Chem.*, 1984, **5**, 129.
48 B. H. Besler, K. M. Merz, Jr. and P. A. Kollman, *J. Comput. Chem.*, 1990, **11**, 431.
49 J. Richardi, P. H. Fries and H. Krienke, *Mol. Phys.*, 1999, **96**, 1411.
50 M. J. Frisch, G. W. Trucks, H. B. Schlegel, G. E. Scuseria, M. A. Robb, J. R. Cheeseman, V. G. Zakrzewski, J. A. Montgomery, R. E. Stratman, J. C. Burant, S. Dapprich, J. M. Millan, A. D. Daniels, K. N. Nudin, M. C. Strain, O. Farkas, J. Tomasi, V. Barone, M. Cossi, R. Cammi, B. Mennucci, C. Pomelli, C. Adamo, S. Clifford, J. Ochterski, G. A. Peterson, P. Y. Ayala, Q. Cui, K. Morokuma, D. K. Malick, A. D. Rabuck, K. Raghavachari, J. B. Foresman, J. Cioslowski, J. V. Ortiz, B. B. Stefanov, G. Liu, A. Liashenko, P. Piskorz, I. Komaromi, R. Gomperts, R. L. Martin, D. J. Fox, T. Keith, M. A. Al-Laham, C. Y. Peng, A. Nanayakkara, C. Gonzalez, M. Challacombe, P. M. W. Gill, B. G. Johnson, W. Chen, M. W. Wong, J. L. Andres, M. Head-Gordon, E. S. Repogle and J. A. Pople, *GAUSSIAN-98*, Gaussian Inc., Pittsburgh, PA, 1998.
51 *Table of Interatomic Distances and Configurations of Ions and Molecules*, The Chemical Society, London, 1958.
52 J. K. Vij, *J. Chem. Phys.*, 1983, **79**, 6182.
53 M. K. Crawford, K. D. Dobbs, R. J. Smalley, D. R. Corbin, N. Maliszewskyj, T. J. Udovic, R. R. Cavanagh, J. J. Rush and C. P. Grey, *J. Phys. Chem. B*, 1999, **103**, 431.
54 B. J. Howard, T. R. Dyke and W. Klemperer, *J. Chem. Phys.*, 1984, **81**, 5417.
55 H. Guo, S. Sirois, E. I. Poroynov and D. R. Salahub, in *Theoretical Treatment of Hydrogen Bonding*, ed. Dusăn Hadži, Wiley, New York, 1997.
56 S. Scheiner, *Hydrogen Bonding, A Theoretical Perspective*, Oxford University Press, Oxford, 1997.
57 D. C. Dayton, K. W. Jucks and R. E. Miller, *J. Chem. Phys.*, 1989, **90**, 2631.
58 I. A. Topol, S. K. Burt and A. A. Rashin, *Chem. Phys. Lett.*, 1995, **247**, 112.
59 R. C. Guedes, B. J. Costa Cabral, J. A. Martinho Simões and H. P. Diogo, *J. Phys. Chem. A*, 2000, **104**, 6062.